CHARGE-TRANSFER COLLISIONS FOR POLARIZED ION SOURCES*

LBL--16300

DE83 015939

Alfred S. Schlachter
Lawrence Berkeley Laboratory, University of California,
Berkeley, CA 94720

Paper presented at the
Workshop on Polarized Proton Ion Sources at TRIUMF
University of British Columbia, Vancouver
May 23-28, 1983.

* This work was supported by the Director, Office of Energy Research, Office of Fusion Energy, Applied Plasma Physics Division of the U.S. Department of Energy under Contract No. DE-AC03-76SF00098.

CHARGE-TRANSFER COLLISIONS FOR POLARIZED ION SOURCES

Alfred S. Schlachter
Lawrence Berkeley Laboratory, University of California,
Berkeley, CA 94720

ABSTRACT

Charge-transfer processes relevant to polarized ion sources are discussed and results are summarized. The primary atom discussed is hydrogen, with particular emphasis on H^- formation. Heavier negative ions are briefly discussed.

INTRODUCTION

Many atomic charge-transfer processes must be understood and atomic data utilized in the design of polarized ion sources, discussed in other papers presented at this conference. Charge-transfer data have been summarized in articles[1-5]; data on charge-transfer in metal-vapor targets have been summarized mainly in conference proceedings.[6-9] This paper contains discussion and summary of charge-transfer processes for hydrogen atoms and ions, primarily in metal-vapor targets, with an emphasis on H^- formation. Formation of metastable H(2s) for Lamb-shift polarized ion sources is also discussed, as are (briefly) formation of He^- and heavier negative ions.

Formation of negative hydrogen ions is of both basic and applied interest: for basic physics research, for injection into accelerators, and for attachment to low-energy atoms for energy analysis. Furthermore, fast H^- can be readily converted to H^0 with high efficiency, with applications to heating of fusion plasmas and to weapons. There are three methods of creating H^- ions: charge transfer, (passage of H^+ or H^0 through a vapor or gas target), surface production (backscattering or desorption of H^- from a low work function surface by ion or atom impact), and "volume" production (direct production of H^- in a discharge). Only charge transfer will be discussed here, since all

H^- polarized ion sources known to the author use charge transfer for the H^- production. (Surface ionization has been used in positive polarized ion sources.) The discussion will concentrate on metal-vapor targets as charge-transfer media, the reason for which can be seen in Fig. 1, which shows the equilibrium yield of H^- for typical gaseous and metal-vapor targets; the metal-vapor targets are a factor of 10 more efficient than are gas targets in converting H^+ or H^0 to H^- at low energies (< 10 keV). There are, of course, other considerations in the selection of a charge-transfer medium, e.g., the energy of the hydrogen beam, scattering in the target, the target thickness required for charge-state equilibrium, target temperature required, and ease of pumping and of handling the target material.

Results for hydrogen and deuterium are intermixed in this paper. Hydrogen and deuterium projectiles at the same velocity have been found to have the same total cross sections and yields over the energy range considered; therefore results for D projectiles will be treated as if the experiment had been performed using H at half the energy, and vice versa. This does not hold for differential cross sections nor for partial cross sections (scattering into or outside of a given angle), for which H and D must be separately considered.

SYSTEMATICS OF CHARGE TRANSFER

This section contains a general discussion of the systematics of charge transfer; the reader is also referred to Refs. 3 and 4 and to the appendix of Ref. 10.

A beam of intensity I_{inc} is incident on a target of thickness τ (Fig. 2). Target thickness τ is the integral of the target density along the beam path:

$$\tau = \int_0^{\ell} n(x)dx \equiv \tau \ell_{eff} \qquad (1)$$

where $n(x)$ is density, x is measured along the beam path, ℓ is the total distance over which $n(x)$ is non-zero, τ is the average

density, and ℓ_{eff} is the effective target length. The beam in Fig. 2 is shown leaving the target in 3 charge states, with intensity I_+, I_0, and I_-. More generally, the fraction of the beam leaving the target in charge state i is $F_i(\tau)$.

$$F_i(\tau) = \frac{I_i(\tau)}{\sum_j I_j(\tau)} \quad . \tag{2}$$

By definition

$$\sum_i F_i(\tau) \equiv 1 \quad . \tag{3}$$

The equilibrium yield, F_i^∞, is the fraction in charge state i of the beam leaving the target relative to the total beam after the target, for a very thick target.

$$F_i^\infty = \lim_{\tau \to \infty} F_i(\tau) \quad . \tag{4}$$

Some experimenters measure the conversion efficiency $\eta_i(\tau)$ rather than $F_i(\tau)$; $\eta_i(\tau)$ is the fraction of beam in charge state i leaving the target relative to the incident beam.

$$\eta_i(\tau) = \frac{I_i(\tau)}{I_{inc}} \quad . \tag{5}$$

For a given geometry, there is some optimum value of τ such that $\eta_i(\tau)$ exhibits a maximum: η_i^{opt}. Because scattered beam can be lost from a target,

$$\Sigma I_i \leq I_{inc}, \tag{6}$$

and

$$\lim_{\tau \to \infty} \eta_i(\tau) = 0 \quad . \tag{7}$$

We have shown in the appendix to Ref. 10 that

$$\eta_i^{opt} \leq F_i^\infty \quad . \tag{8}$$

Also, F_i^{∞} is independent of target geometry, while η_i^{opt} is dependent on the geometry of the target.

A schematic example showing fluxes and charge-state fractions for a typical 3-state system is shown in Figs. 3a and 3b. The equilibrium charge-state fractions are apparent in Fig. 3b, while optimum fluxes (equivalent to η_i^{opt}) are evident in Fig. 3a.

There are certain (unusual) 3-state systems in which F_i exhibits an optimum value (Fig. 4a). An example is the fraction F_0 for fast H^- incident on a target; F_0 is optimal for some value of π, then decreases with further increase of target thickness.

Charge transfer for a 4-state system is often different, especially when one or more states is fragile, i.e., the fragile state is generated only from a particular state which disappears after several collisions, while the fragile state itself is readily destroyed in collisions subsequent to its formation (Fig. 4b). An example of a 4-state system is hydrogen including the metastable 2s state: H^+, $H^0(1s)$, $H^0(2s)$, and H^-. H(2s) is the fragile charge state; it is created by electron capture of low-energy H^+ in a metal vapor, and is quenched (de-excited) in subsequent collisions. Another example is helium, in which 4 states[11] are considered: He^+, $He^0(t)$, $He^0(s)$, and He^-, where $He^0(t)$ and $He^0(s)$ are atoms in triplet and singlet states. The $He^0(t)$ and He^- are both fragile.

Two related quantities are referred to for metastable H(2s): f_{2s} and F_{2s} or f_m and F_m). F_{2s} is the fraction of total beam leaving the target in the metastable 2s state, consistent with the definition in Eq. 2, while f_{2s} is the fraction of neutral atoms in the metastable 2s state.

Cross sections, charge-state fractions, and equilibrium yields are related by a set of coupled linear first-order differential equations:

$$\frac{dF_i}{d\pi} = \Sigma F_j \sigma_{ji} - \Sigma F_i \sigma_{ij} \quad . \tag{9}$$

For n states there are n(n-1) cross sections, e.g., 2 cross sections for 2 states, 6 for 3 states, and 12 for 4 states. Solutions to Eq. 9 can be found analytically[3,4] or by numerical integration.

A particularly simple and useful result is obtained for 2 states:

$$F_i^- = \frac{\sigma_{ji}}{\sigma_{ji} + \sigma_{ij}}$$

and

$$F_j^- = \frac{\sigma_{ij}}{\sigma_{ji} + \sigma_{ij}} \quad . \tag{10}$$

For the case of F_0 and F_-, Eq. 10 becomes

$$F_-^- = \frac{\sigma_{0-}}{\sigma_{0-} + \sigma_{-0}}$$

and

$$F_0^- = \frac{\sigma_{-0}}{\sigma_{0+} + \sigma_{-0}} \quad . \tag{11}$$

EXPERIMENTAL APPROACH

A typical experimental apparatus[10] for measurement of charge transfer in an alkali-metal vapor target is shown in Fig. 5. A momentum-analyzed beam of D^+(or H^+) is incident from the left. The target is a heat pipe, designed to recirculate alkali metal to minimize loss out the ends of the target. Use of a heat pipe for Cs, Rb, and Na is described in detail in Ref. 10. The beam after the collision is charge-state analyzed in a transverse electric field. The D^+ and D^- are detected by magnetically-suppressed Faraday cups, while the D^0 beam is detected with a

pyroelectric detector.[10, 12-14] Detection of the D^0 beam is the aspect of the experiment most subject to uncertainty in the measurement of equilibrium yields. The pyroelectric detector is linear, sensitive (~1V/Watt), and its response is independent of the charge state of the projectile hitting it, hence it can be calibrated with an ion beam of known intensity. The D^+ beam incident on the target is modulated, and the AC voltage generated on the pyroelectric detector is measured with a lock-in amplifier. Details can be found in Refs. 10 and 12-14.

A heat pipe cannot be used for alkaline-earth vapors in the density range of interest for charge transfer, because the melting temperature of the alkaline earth is higher than the operating temperature of the target. A typical design of a target[12] used for alkaline-earth vapors is shown in Fig. 6. An iron oven is heated by quartz lamps to obtain the temperature required, typically 400-800°C.

Data for 1-keV D^+ incident on cesium vapor[10] and for 3-keV D^+ on barium vapor[12] are shown as a function of target thickness or number density in Figs. 7 and 8. Charge-state equilibrium is apparent in both cases. Also shown in each figure is total beam transmitted through the target. It should be noted that the angle defined by the exit aperture of the alkaline-earth target was about half that of the alkali-metal target, so transmitted beam cannot easily be compared. Figure 7 also shows[15] the fraction F_{2s}, i.e., the metastable-atom fraction of the beam (as well as F_0, the total neutral fraction of the beam), showing that H(2s) play no role in production of H^- in a thick cesium-vapor target.

A major difficulty in measuring equilibrium yields is measurement of the flux of atoms, as discussed above. Minor difficulties include insufficient target thickness, unequal collection efficiency for scattered beams, and assorted problems related to the metal vapor. Cross-section measurements are generally more difficult; the major problems are (1) measurement of the atom flux, (2) incomplete collection and detection of scattered beams, and

(3) measurement of target thickness (usually measurement of the mean target density and effective path length). An additional difficulty in the measurement of H(2s) or H(2p) formation is the detection and collection efficiency of the Lyma-alpha detector. Measurement of 2-electron-transfer cross sections is complicated by the background single-step process (beam contamination) and the competition of two single-step processes.

RESULTS: ALKALI TARGETS

A selection of cross-section and thick-target results for H atoms in alkali-metal vapor targets is presented here. The emphasis is on new and/or otherwise interesting results; more complete results can be found in Refs. 6-10, 12, 16, and the references therein.

The cross sections σ_{+0}, σ_{+-}, and σ_{-+} for D and H in cesium vapor are shown[6] in Fig. 9. Calculated cross sections σ_{+0} by Kimura et al.[17] in cesium and in sodium are shown in Figs. 10 and 11. Figures 10 and 11 show calculations of electron capture from both ground-state and optically excited targets; electron capture from Na*(3p) is seen to be larger than from Na(3s) at low energies. Experiment and calculations for σ_{0-} and σ_{-0} are shown[8, 10] in Figs. 12 and 13. The large values of σ_{+0} and σ_{0-} for H in cesium and the small value of σ_{+-} shows that H^- formation is dominated by the 2-step process, and that direct formation of H^- from H^+ is almost negligible. Calculated cross sections σ_{-0} by Olson and Liu are shown in Fig. 14, showing also the contribution (dashed line) due to electron transfer rather than electron detachment.

The effect of angular scattering in various collision processes has been calculated by Olson and colleagues. Figure 15 shows[19] the acceptance angle needed to collect 50 percent and 90 percent of H^- produced by collision of H^0 in cesium. Elastic scattering of H^0 is an important process in charge transfer. Olson has calculated the percent of σ_{00} (elastic scattering)

outside a given angle for H^0 in cesium (Fig. 16) and in sodium[7] (Fig. 17).

Lamb-shift polarized ion sources require a beam of H atoms in the metastable 2s state. Selective electron capture[20] is required to form H^- from polarized H(2s).

Formation of the metastable H(2s) state for H^+ incident on alkali-metal vapors has been studied in a number of experiments,[15, 21-23] usually by de-excitation of the H(2s) (quenching) in an applied electric field. The resulting Lyman-alpha radiation is polarized. Cross sections σ_{+m} and σ_{+r} (formation of the metastable 2s state and the radiative 2p state) has been measured in cesium by Pradel et al.[15] shown in Fig. 18; the metastable fraction F_{2s} of the total beam for H^+ in cesium as a function of target thickness τ is shown[15] in Fig. 19. A summary of measurements of the fraction f_{2s} of metastable H(2s) relative to the neutral beam is shown in Fig. 20. We see that both σ_{+m} and f_{2s} show a peak at about 500eV for H^+ in cesium vapor, and that f_{2s} is large, of the order of 30-50 percent. Similar results by Nagata[23] are shown in Fig. 21 for other alkali vapor targets.

The equilibrium yield $F_-^=$ for D^- and H^- formation in cesium vapor is summarized[10] in Fig. 22; optimum conversion efficiency η^{opt} in cesium is shown in Fig. 23. The yield $F_-^=$ in cesium vapor is seen to be large: 20-35 percent at low energies. Similar results[10] for sodium vapor are shown in Fig. 24 and 25; the yield $F_-^=$ is seen to be of the order of 10 percent at intermediate energies.

The equilibrium yield can be compared with cross sections using Eq. 11. This is shown for cesium vapor[10] in Fig. 26; measured $F_-^=$ is seen to agree with $F_-^=$ calculated from cross sections.

RESULTS: ALKALINE-EARTH TARGETS

Recent results for $F_-^=$ in alkaline-earth vapor targets are

summarized in Ref. 12, in which a maximum F_- of 50 percent is reported for charge transfer in a thick strontium-vapor target at an energy of 250eV/amu. Results by different experimental groups are in excellent agreement for alkaline-earth vapor targets. An example is shown in Fig. 27, which shows three measurements of F_- in strontium vapor.

Cross sections for charge transfer in alkaline-earth vapors have recently been measured[24]; results for σ_{0-}, σ_{+-}, σ_{0+}, and σ_{0-} are shown in Figs. 28-31, along with σ_{-0} deduced from F_- measurements and Eq. 11 It is to be noted that σ_{0-} increases with decreasing energy in strontium vapor, while σ_{-0} is relatively flat with energy, which is responsible for the large value of F_- in strontium vapor at low energy.

Formation of H(2s) by collisions of H^+ in alkaline-earth vapors has been reported.[25] Results are shown in Figs. 32-33.

SUMMARY: H^- FORMATION

Results for F_- in various alkali and alkaline-earth vapors are shown[12] in Fig. 34. Strontium vapor gives an F_- of as large as 50 percent at an energy of 250 eV/amu. Cesium gives 35 percent at lower energies, rubidium gives a high yield at intermediate energies, and sodium gives the highest yield for energies above 2 keV/amu.

HEAVIER NEGATIVE IONS

Formation of He^- by charge transfer in a metal vapor[26] requires consideration of (at minimum) a 4-state system. The He^- ion is a quartet state; it is created by electron capture of a helium atom in a triplet state. Both the $He^0(t)$ and He^- fractions show optimum values, and are very small for thick targets. Results[26] are shown in Figs. 35 and 36; Fig. 37 shows that the maximum F_-^{opt} for He^- in cesium is 1.4 percent at 6 keV.

Formation of heavier negative ions has been surveyed[27] in sodium and magnesium vapor targets. Results are shown in Figs. 38 and 39. Yields approaching 100 percent are possible for favorable cases.

SUMMARY

Recent theoretical calculations and experimental results are providing a coherent understanding of H^- formation by charge transfer in metal vapors, although some disagreement exists between different experimental results or between experimental and theory in a few cases. The H^- yield is especially large in cesium vapor at low energies, exceeding 30 percent for energies below 400 eV/amu, and in strontium vapor, where the yield is 50 percent at 250 eV/amu. Charge transfer leading to formation of metastable H(2s) and to He^- and other heavier negative ions is briefly discussed. Additional considerations for application of charge transfer to polarized ion sources, e.g., angular scattering of beams, are also mentioned. The data and references in this report should be useful for the design of polarized ion sources requiring charge transfer.

ACKNOWLEDGMENT

I would like to acknowledge Catherine Searle for her assistance in editing this manuscript. This work was supported by the Director, Office of Energy Research, Office of Fusion Energy, Applied Physics Division of the U. S. Department of Energy under Contract No. DE-AC03-76SF00098.

REFERENCES

1. C. F. Barnett, J. A. Ray, E. Ricci, M. I. Wilken, E. W. McDaniel, E. W. Thomas, and H. B. Gilbody, "Atomic Data for Controlled Fusion Research," ORNL-5206 and ORNL-5207, (1977).
2. Y. Kaneko, T. Arikawa, Y. Itikawa, T. Iwai, T. Kato, N. Matsuzawa, Y. Nakai, K. Okuno, H. Ryufuku, H. Tawara, and T. Watanabe, "Cross Sections for Charge Transfer Collisions Involving Hydrogen Atoms," IPPJ-AM-15, Nagoya University, (1980).
3. S. K. Allison, "Experimental Results on Charge-changing Collisions of Hydrogen and Helium Atoms and Ions at Kinetic Energies above 0.2 keV," Rev. Mod. Phys. 30, 1137 (1958).
4. H. Tawara and A. Russek, "Charge Changing Processes in Hydrogen Beams," Rev. Mod. Phys. 45, 178 (1973); H. Tawara, "Cross Sections for Charge Transfer of Hydrogen Beams in Gases and Vapors in the Energy Range 10eV to 10keV," Atomic Data and Nuclear Data Tables, 22, 491(1978).
5. Y. Nakai, A. Kikuchi, T. Shirai, and M. Sataka," Data on Collisions of Hydrogen Atoms and Ions with Atoms and Molecules (1)," JAERI-M 83-013, Japan Atomic Energy Research Institute, 1983.
6. A. S. Schlachter, "D^- Production by Charge Transfer in Metal Vapors," in Proceedings of the Second International Symposium on the Production and Neutralization of Negative Hydrogen Ions and Beams, edited by Th. Sluyters, (Brookhaven National Lab., Upton, 1980), pp. 42-50 (BNL-51304). Also, LBL-11635, Lawrence Berkeley Laboratory.
7. R. E. Olson, "Theoretical Investigations of the Collision Dynamics in H^- Formation and Destruction," ibid., pp. 51-57.
8. A. S. Schlachter, "Production and Destruction of D^- by Charge Transfer in Metal Vapors", in Proceedings of the U.S. Mexico Joint Seminar on the Atomic Physics of Negative Ions, edited by I. Alvarez and C. Cisneros, Notas de Fisica 5 (1982) (Instituto de Fisica, UNAM, Mexico), pp. 481-516. Also, LBL-12995, Lawrence Berkeley Laboratory.

9. R. E. Olson, "Molecular Negative Ions," ibid., pp. 78-107.
10. A. S. Schlachter, K. R. Stalder, and J. W. Stearns, Phys. Rev. A 22, 2494 (1980).
11. Both hydrogen and helium have more than 4 charge states; this simplication is, nonetheless, often useful.
12. R. H. McFarland, A. S. Schlachter, J. W. Stearns, B. Liu, and R. E. Olson, Phys. Rev. A 26, 775 (1982).
13. K. H. Berkner, B. R. Meyers, and R. V. Pyle, Rev. Sci. Instrum. 39, 1204 (1968).
14. M. W. Geis, K. A. Smith, and R. D. Rundel, J. Phys. E 8, 1011 (1975).
15. P. Pradel, F. Roussel, A. S. Schlachter, G. Spiess, and A. Valance, Phys. Rev. A 10, 797 (1974).
16. L. W. Anderson, T. J. Morgan, R. E. Olson, A. S. Schlachter, and J. W. Gallagher, Atomic Data and Nuclear Data Tables (article in preparation).
17. M. Kimura, R. E. Olson, and J. Pascale, Phys. Rev. A 26, 3113 (1982).
18. R. E. Olson and B. Liu, J. Chem. Phys. 73, 2817 (1980).
19. R. E. Olson, Phys. Lett. 77A, 143 (1980).
20. B. Donnally and W. Sawyer, Phys. Rev. Lett. 15, 439 (1965); F. Roussel, P. Pradel, and G. Spiess, Phys. Rev. A 16, 1854 (1977); Phys. Rev. A 15, 451(1977); and references therein.
21. V. N. Tuan, G. Gautherin, and A. S. Schlachter, Phys. Rev. A 9, 1242 (1974).
22. F. Brouillard, W. Claeys, and G. Van Wassenhove, J. Phys. B 10, 687 (1977); and X ICPEAC (Paris, 1977), pp. 1264-5.
23. T. Nagata, J. Jpn. Phys. Soc. 46, 1622 (1979).
24. M. Mayo, J. Stone, and T. J. Morgan, 1983 (in press).
25. T. J. Morgan and F. Eriksen, Phys. Rev. A 19, 2185 (1979).
26. A. S. Schlachter, D. H. Loyd, P. J. Bjorkholm, L. W. Anderson, and W. Haeberli, Phys. Rev. A 174, 201 (1968).
27. J. Heinemeier and P. Hvelplund, Nucl. Instrum. Meth. 148, 65 (1978); 148, 425 (1978).

28. Y.A.Agafonov, B.A.D'yachkov, and M.A.Pavlii, Pis'ma Zh.Tekh. Fiz. 2, 757 (1976) (Sov.Tech.Phys.Lett. 2, 296 (1976)).
29. Y.A.Agafonov, B.A.D'yachkov, and M.A.Pavlii, Sov.Phys.-Tech. Phys. 25, 1261(1980).
30. C. J. Anderson, R. J. Girnius, A. M. Howald, and L. W. Anderson, Phys. Rev. A 22, 822 (1980); R. J. Girnius, C. J. Anderson, and L. W. Anderson, Phys. Rev. A 16, 2225 (1977).
31. C. J. Anderson, A. M. Howald, and L. W. Anderson, Nucl. Instrum. and Methods 165, 583 (1979).
32. H. Bohlen, G. Clausnitzer, and H. Wilsch, Z. Phys. 208, 159 (1968).
33. K. H. Berkner, D. Leung, R. V. Pyle, A. S. Schlachter, and J. W. Stearns, Nucl. Instrum. and Methods 143, 157 (1977); Phys. Lett. 64A, 217 (1977).
34. C. Cisneros, I. Alvarez, C. F. Barnett, and J. A. Ray, Phys. Rev. A 14, 76 (1976).
35. K. Miethe, C. Achenbach. T. Dreiseidler, A. Muller, and E. Salzborn, in Proceedings of the European Conference on Atomic Physics, edited by J. Kowalski, G. zu Pulitz, and H. G. Weber (Heidelberg, 1981), pp. 997-998 (Europhysics Conference Abstracts, Volume 5A); Klaus Miethe, Doctoral Thesis, Universitat Giessen, 1981 (unpublished); and private communication.
36. G. I. Dimov and G. V. Roslyakov, Prib. Tekh. Eksp. 3, 31 (1974) [Instrum. Exp. Tech. 17, 658 (1974)].
37. B. A. D'yachkov and V. I. Zinenko, At. Energ. 24, 18 (1966) [Sov. At. Energ. 24, 16 (1968)]; B. A. D'yachkov, V. I. Zinenko, and M. A. Pavlii, Zh. Tekh. Fiz. 41, 2353 (1971) [Sov. Phys. - Tech. Phys. 16, 1868 (1972)].
38. R. J. Girnius, L. W. Anderson, and E. Staab, Nucl. Instrum. and Methods 143, 505 (1977).
39. W. Gruebler, P. A. Schmelzbach, V. Konig, and P. Marmier, Phys. Lett. A 29, 440 (1969); Helv. Phys. Acta 43, 254 (1970).
40. J. R. Hiskes, A. M. Karo, P. A. Willman, and W. J. Stevens, Phys. Let. 68A, 221 (1978).

41. R. N. Il'in,. V. A. Oparin, E. S. Solv'ev and N. V Fedorenko, Zh. Eksp. Teor. Fiz. Pis'ma Red. 2, 310 (1965) [JETP Lett. 2, 197 (1965))]; Zh. Tekh, Fiz. 36, 1241 (1966)[Sov. Phys. - Tech. Phys. 11, 921 (1967)]; R. N. Il'in, V. AS. Oparin, I. T. Serenkov, E. S. Solov'ev and N. V. Fedorenko, Proc. VII Intl. Conf. on Phys. of Electronic and Atomic Collisions, Amsterdam, 1971, L. M. Branscomb et al, Editors (North-Holland Publishing Co., Amsterdam, 1971), v. 2, p. 793.

42. R. K. Janev and Z. M Radulovic, Phys. Rev. A 17, 889 (1978).

43. Yu. M. Khirnyi, and L. N. Kochemasova, Prib. Tekh. Eksp. 3, 56 (1970) [Instrum. Exp. Tech. 3, 693 (1970)].

44. T. E. Leslie, K. P. Sarver, and L. W. Anderson, Phys. Rev. A 4, 408 (1971). These results as plotted have been renormalized (multipled by 2.0) to take into account more recent measurements of σ_{+0}.

45. F.W.Meyer, Rev. Sci, Instrum. 51, 1295 (1980); J.Phys.B 13, 3823 (1980).

46. F. W. Meyer and L. W. Anderson, Phys. Rev. A 11, 589 (1975); Phys. Lett. 54A, 333 (1975); F. W. Meyer, C. J. Anderson, and L. W. Anderson, Phys. Rev. A 15, 455 (1977).

47. T. J. Morgan, J. Stone, M. Mayo, and J. Kurose, Phys. Rev. A 20, 54 (1979).

48. T. Nagata in Proc. XI Int. Conf. on Phys. of Electronic and Atomic Collisions, edited by K. Takayanagi and N. Oda (Kyoto, Japan 1979). pp. 512-513; J. Phys. Soc. Japan 46, 919 (1979); J. Phys. Soc. Japan 48, 2068 (1980), and private communication.

49. R.E.Olson, E.J.Shipsey, and J.C.Browne, Phys.Rev. A 13, 180 (1976). The values for σ_{0-} cited should be divided by four (R.E.Olson, private communcation).

50. A. S. Schlachter, P. J. Bjorkholm, D. H. Loyd, L. W. Anderson, and W. Haeberli, Phys. Rev. 177 184 (1969).

51. G. Spiess, A. Valance, and P. Pradel, Phys. Rev. A 6 746 (1972).

REFERENCES TO DATA IN FIGURES

ADP 76	Agafanov, D'yachkov, and Pavlii (1976)[28]
ADP 80	" " " (1980)[29]
AGHA	Anderson, Girnius, Howald and Anderson (1977-1980)[30]
AHA	Anderson, Howald, and Anderson (1979)[31]
BCW	Bohlen, Clausnitzer, and Wilsh (1968)[32]
BLPSS	Berkner, Leung, Pyle, Schlachter, and Stearns (1977)[33]
BVC	Brouillard, Claeys, and VanWassenhove (1977)[22]
CABR	Cisneros, Alvarez, Barnett, and Ray (1976)[34]
DMS	Dreiseidler, Miethe, and Salzborn (1981)[35]
DR	Dimov and Roslyakov (1974)[36]
DZP	D'yachkov, Zinenko, and Pavlii (1966-1971)[37]
GAS	Girnius, Anderson, and Staab (1977)[38]
GSKM	Gruebler, Schmelzbach, Konig, and Marmier (1969, 1970)[39]
HKWS	Hiskes, Karo, Willman, and Stevens (1978)[40]
IOSF	Il'in, Oparin, Solov'ev, and Fedorenki (1965-1971)[41]
JR	Janev and Radulovic (1978)[42]
KK	Khirnyi and Kochemasova (1970)[43]
LSA	Leslie, Sarver, and Anderson (1971)[44]
M	Meyer (1980)[45]
MA	Meyer and Anderson (1975-1977)[46]
MSMK	Morgan, Stone, Mayo, and Kurose (1979)[47]
N	Nagata (1979-1980)[48]
N79a	Nagata (1979)[23]
O	Olson (1980)[19]
OL	Olson and Liu (1980)[18]
OSB	Olson, Shipsey, and Browne (1976)[49]
PRSSV	Pradel, Roussel, Schlachter, Speiss, and Valance 1974)[15]
SBLAH	Schlachter, Bjorkholm, Loyd, Anderson, and Haeberli (1969)[50]
SSS	Schlachter, Stalder, and Stearns (1980)[10]
SVP	Spiess, Valance, and Pradel (1972)[51]
TGS	Tuan, Gautherin, and Schlachter (1974)[21]
VBC	VanWassenhove, Brouillard, and Claeys (1977)[22]

Figure Captions

1. Summary of equilibrium yield F_i^∞ for H in typical metal vapors (Sr, Cs, Na) and gases (H_2, Xe).

2. Schematic diagram of experiment to measure charge-state fractions. A flux I_{inc} is incident on a target of thickness π. Fluxes I_+, I_0, and I_- in charge states +,o, and - leave the target.[8]

3. Schematic behavior of currents and charge-state fractions as a function of target thickness π for a 3-state system (+,o, and -) with the incident beam in charge-state +. Figure 3a shows currents I_i, indicating optimum values of the o and - charge states; Fig. 3b shows charge-state fractions F_i, indicating equilibrium values. An example is low-energy H^+ incident on an alkali-vapor target.

4. Schematic behavior of charge-state fractions F_i as a function of target thickness π for 2 systems having an F_0^{opt}. Figure 4a shows an unusual 3-state system, e.g., fast H^- incident on a gas target; the F_0 fraction shows an optimum value. Figure 4b shows moderate energy He^+ incident on a metal-vapor target; the fractions $F_0(m)$ and F_- both have an optimum value.

5. Schematic diagram of apparatus used by the LBL group[10] to measure charge-state fractions in alkali-metal vapors. A heat-pipe target is shown. A transverse electric field is used to charge-state analyze the beam after the target; Faraday cups are used to detect the D^+ and D^- ions, and a pyroelectric detector is used to detect the D^0 atoms.

6. Schematic diagram of apparatus used by the LBL group[12] to measure charge-state fractions in alkaline-earth vapors. The target was heated by quartz lamps.

7. Charge-state fractions, F_i, as a function of cesium-target thickness, π, for 1-keV D^+ incident on cesium vapor.[10] Also shown are charge-state fractions including the fraction in the metastable D(2s) state measured by Pradel et al.,[11] and the total beam transmitted through the target.[10]

8. Charge-state fractions F_i and total transmitted beam as a function of target number and line densities for 3-keV D^+ incident on barium vapor.[12] Line density has an uncertainty of 50 percent.

9. Cross sections for D ions and atoms in cesium vapor.[6]

10. Electron-capture cross sections for $H^+ + Cs(6s)$ (solid lines) and $H^+ + C^*(6p)$ collisions (dashed lines), calcula-

ted by Kimura et al.[17] The heavy solid and dashed lines belong to the total capture cross sections. The detailed H(2s) and H(2p) cross sections are labeled. Experimental cross sections of Nagata[48] are given by solid circles for total electron capture and by solid triangles for H(2s) production for collisions of H^+ with ground state Na(3s).

11. Calculated electron-capture cross sections for H^+ + Na(3s) collisions (solid lines) and H^+ + Na* (3p) collisions (dashed lines) calculated by Kimura et al.[17] Same notation as in Fig. 10.

12. Cross section σ_{0-} for deuterium in cesium vapor.[8,10] Experimental results are shown as points, calculations as lines.

13. Cross section σ_{-0} for deuterium in cesium vapor.[8,10] Experimental results are shown as points, calculation as lines.

14. Cross section σ_{-0} calculated by Olson and Liu[18] for the electron-loss reactions H^- + Alk → H^0 + .. where Alk ≡ Na, K, Rb, and Cs (solid lines). The components of the electron loss that are due to electron transfer, H^- + Alk→H^0 + Alk^-, are given by the dashed lines. The difference between the above cross sections represents direct detachment of the H^+ + Na + e^- continuum and production of autodetaching states of H^+Na^{-*}.

15. Calculation of acceptance angle required to observe 50 percent or 90 percent of the negative ion formation for H^0 on cesium, calculated by Olson.[19] The calculations on H^- production in H^0 + Cs collisions are given by solid lines while the measurements of Cisneros et al.[34] for D^- production in D^+ Cs collisions are given by dashed lines.

16. Percent of the total elastic cross sections found outside various angles for the H^0 + Cs collision system, calculated by Olson.[7]

17. Precent of the total elastic cross section found outside various angles for the H^0 + Na collision system, calculated by Olson.[7]

18. Cross sections σ_{+m} and σ_{+r} for protons in cesium vapor, measured by Pradel et al.[15] σ_{+m} is the cross section for electron capture in the metastable 2s state, σ_{+r} for electron capture in the radiative 2p states. O: incident H^+; ●: incident D^+ (shown at equivalent H^+ velocity).

19. H(2s) fractional yield as a function of Cs target thickness x for incident H^+ energies between 0.5 and 2.5 keV, measured by Pradel et al.[15] The H(2s) fraction shown in this figure is the fraction of outgoing beam in the 2s state relative to

the total outgoing beam; ordinate corresponds to a 10 percent fractional yield.

20. Summary of measurements of metastable atom fraction f_{2s} in neutral beam for H^+ in cesium vapor.

21. Metastable atom fraction f_{2s} in neutral beam for H^+ in alkali vapors, measured by Nagata.[23]

22. Equilibrium yield, $F_=$, for D in cesium vapor.[10]

23. Optimum negative-ion conversion efficiency, $\eta_=^{opt}$, for D in cesium vapor.[10]

24. Equilibrium yield, $F_=$, for D in sodium vapor.[10]

25. Optimum negative-ion conversion efficiency, $\eta_=^{opt}$, for D in sodium vapor.[10]

26. Equilibrium yield, $F_=$, for D in cesium vapor, comparing direct measurement with yield calculated from cross sections (Eq. 11).[8]

27. Equilibrium yield, $F_=$, for D in strontium vapor.[12]

28. Single-electron-capture cross sections σ_{10} for collisions of H^+ with Mg,[25] Ba,[25] Sr and Ca[24] vapor targets, measured by Mayo et al.[24]

29. Double-electron capture cross sections σ_{1-1} for collisions of H^+ with Mg,[25] Ba,[25] and Sr and Ca[24] vapor targets, measured by Mayo et al.[24]

30. Single-electron capture, σ_{0-1} and loss, σ_{01}, cross sections for collisions of H^0 with Sr, measured by Mayo et al.[24]

31. Electron-detachment cross section σ_{-10} for H^- in collisions with Ca and Sr vapor targets. ●, Ca target; O, Sr target, inferred from σ_{0-} and $F_=$ measurements.[24]

32. Cross section for formation of H(2s) atoms in Ar, He, Ba, and Mg targets reported by Morgan and Eriksen.[25]

33. H(2s) metastable atom fraction of the neutral beam as a function of proton energy for Cs, Mg, and Ba targets, reported by Morgan and Eriksen.[25]

34. Summary of equilibrium yield, $F_=$, for H in Sr, Ca, Cs, Ba, Rb, Mg, and Na vapors.[12]

35. Charge-state fractions for 25-keV He^+ in cesium vapor[25] as a function of target thickness τ.

36. Computed fractions of atoms in singlet states and triplet states for 25-keV He^+ in cesium vapor.[26]

37. Maximum yield of He^- ions for He^+ in cesium vapor.[26]

38. Measured negative equilibrium yield vs. energy for various projectiles in sodium vapor (electron affinities in eV given in brackets) reported by Heinemeir and Hvelplund.[27]

39. Measured negative equilibirium yeild vs. energy for various projectiles in magnesium vapor (electron affinities in eV given in brackets) reported by Heinemeier and Hvelplund.[27]

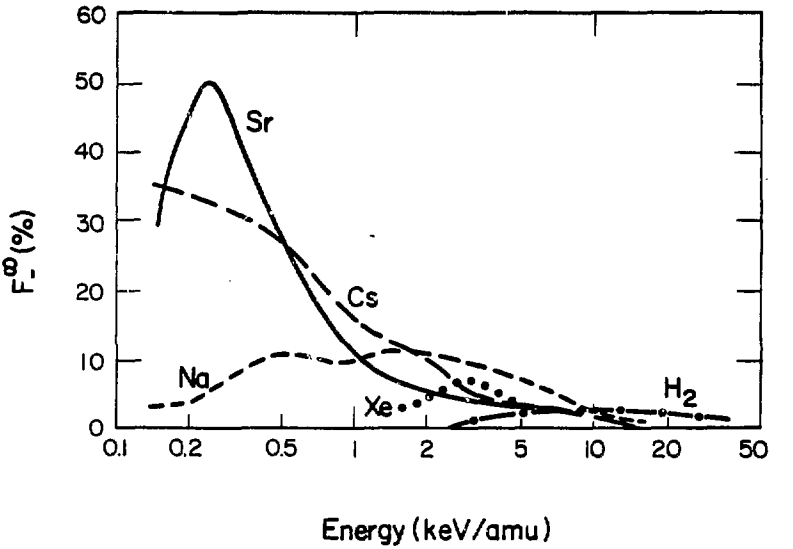

XBL 836-2684

FIGURE 1

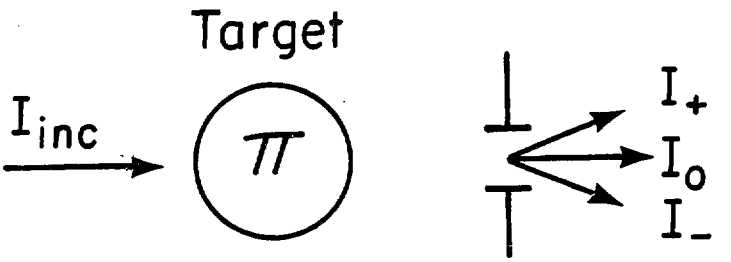

XBL 815-2283

FIGURE 2

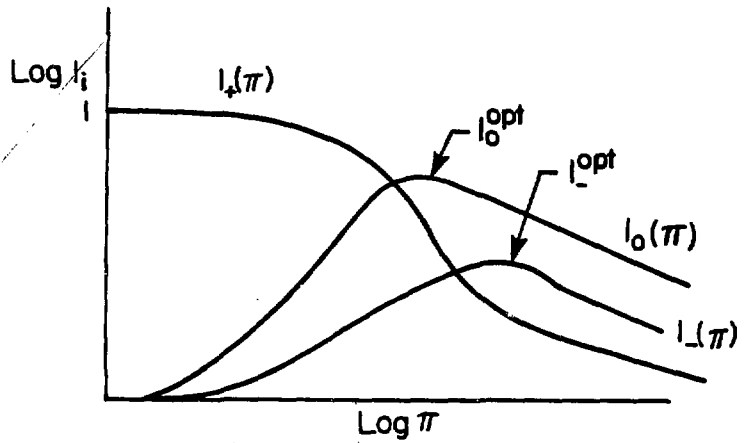

XBL 836-10265

FIGURE 3A

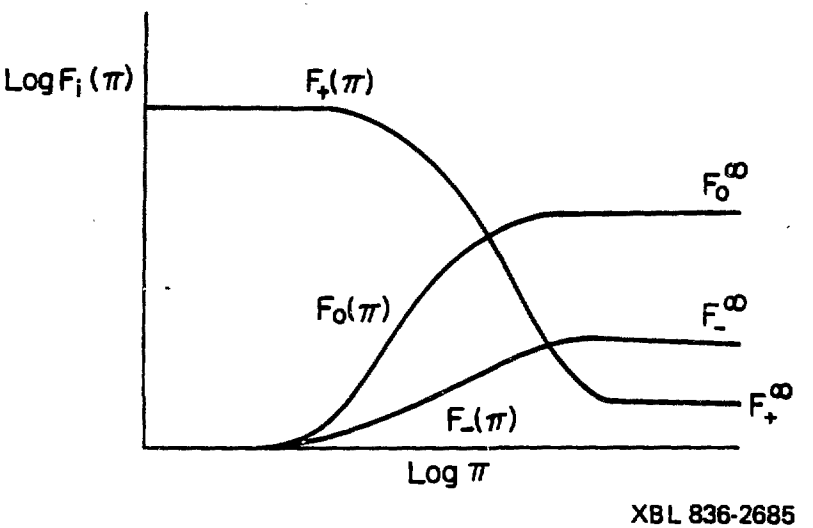
Log $F_i(\pi)$
$F_+(\pi)$
F_o^∞
$F_o(\pi)$
F_-^∞
$F_-(\pi)$
F_+^∞
Log π
XBL 836-2685

FIGURE 3B

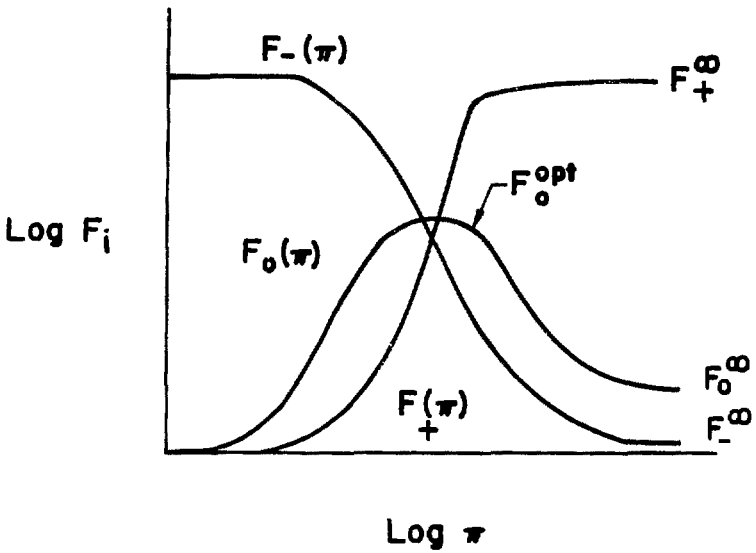

XBL 836-10264

FIGURE 4A

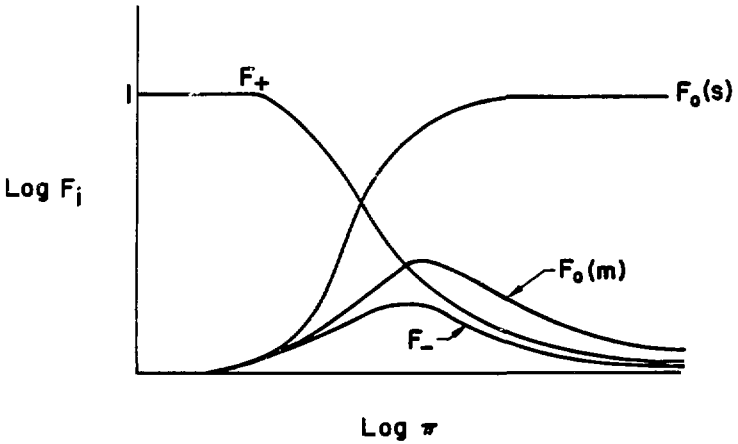

XBL 836-10263

FIGURE 4B

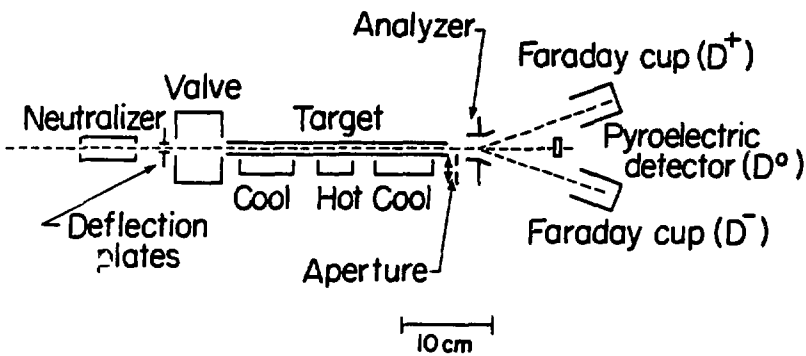

XBL 7811-12779A

FIGURE 5

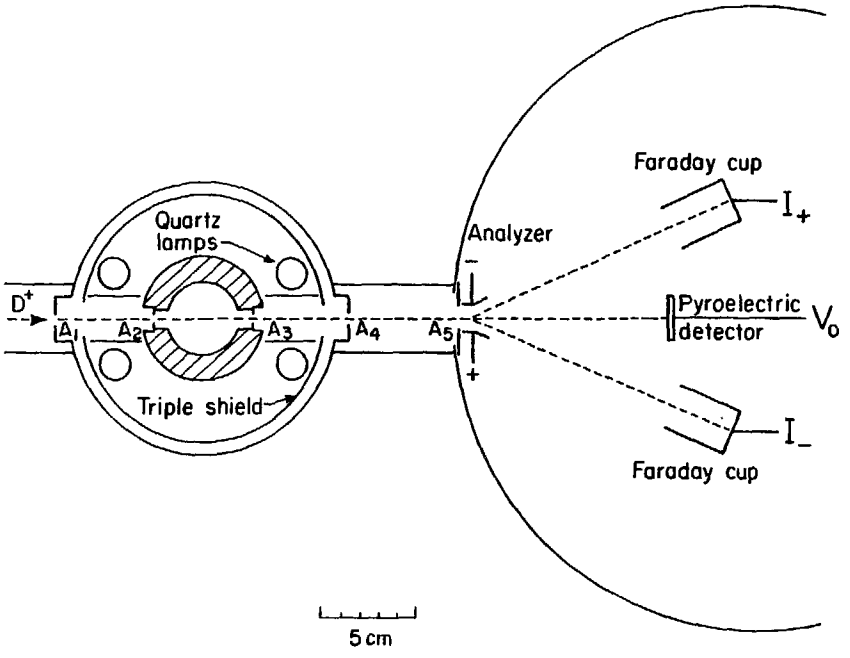

XBL 813-2182A

FIGURE 6

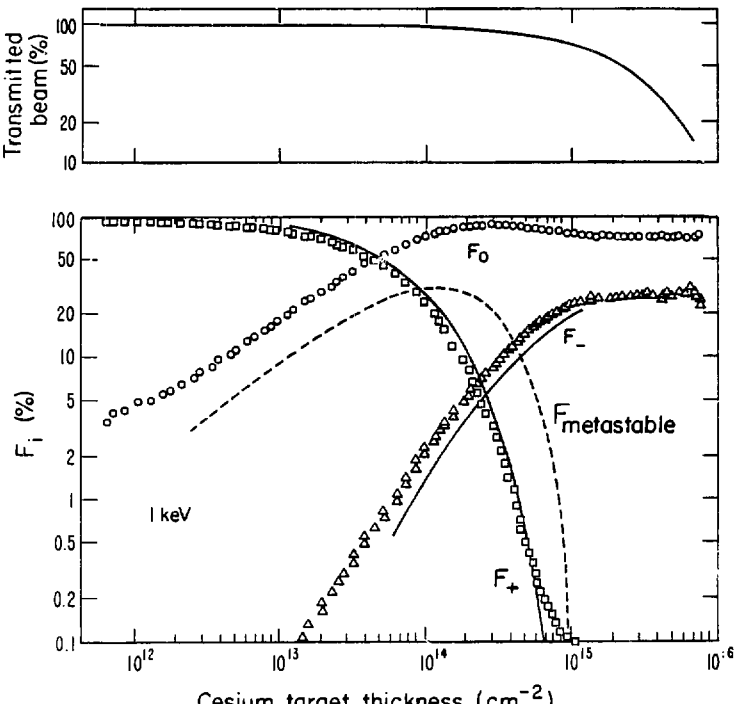
Transmitted beam (%)
100
50
20
10
F_i (%)
100
50
20
10
5
2
1
0.5
0.2
0.1
F_0
F_-
$F_{metastable}$
F_+
1 keV
10^{12}
10^{13}
10^{14}
10^{15}
10^{16}
Cesium target thickness (cm^{-2})
XBL815-2295

FIGURE 7

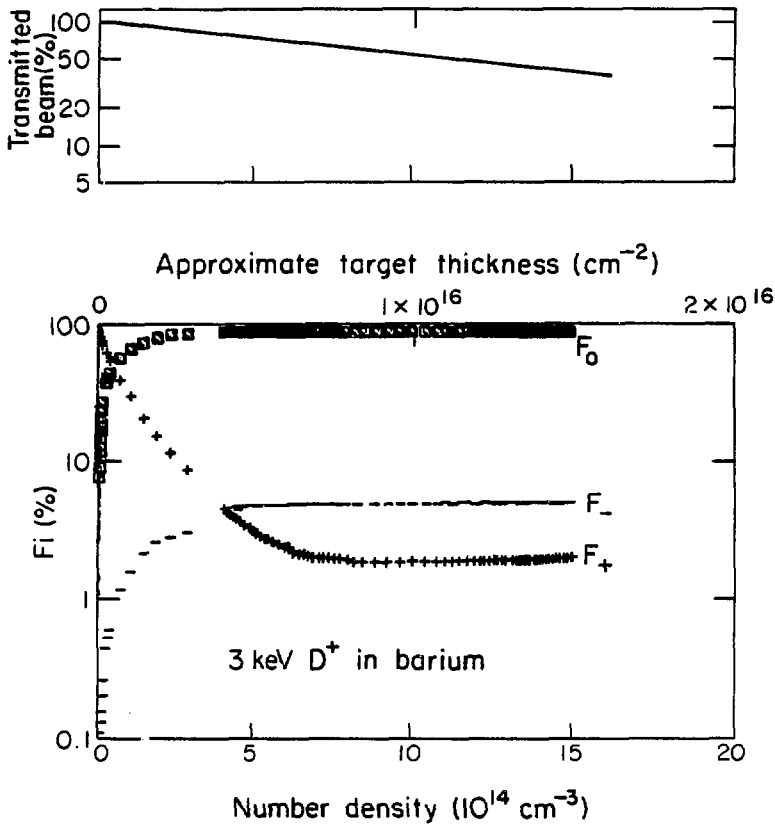
Transmitted beam(%)
100
50
20
10
5
Approximate target thickness (cm^{-2})
0
1×10^{16}
2×10^{16}
100
10
1
0.1
Fi (%)
F_0
F_-
F_+
3 keV D^+ in barium
0
5
10
15
20
Number density (10^{14} cm^{-3})
XBL 815-2286B

FIGURE 8

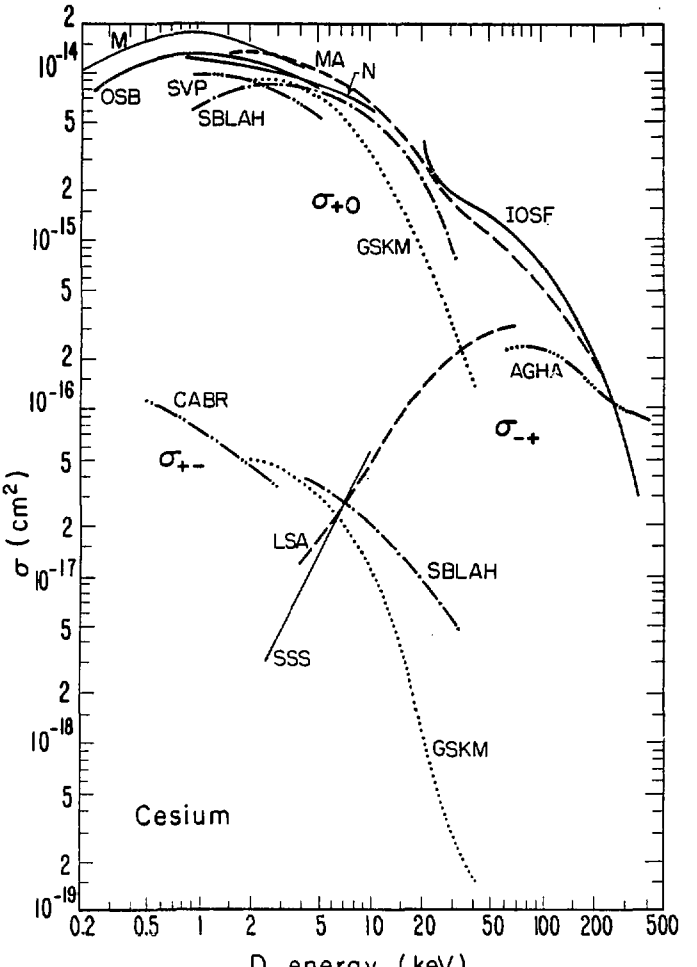

XBL 809-2007

FIGURE 9

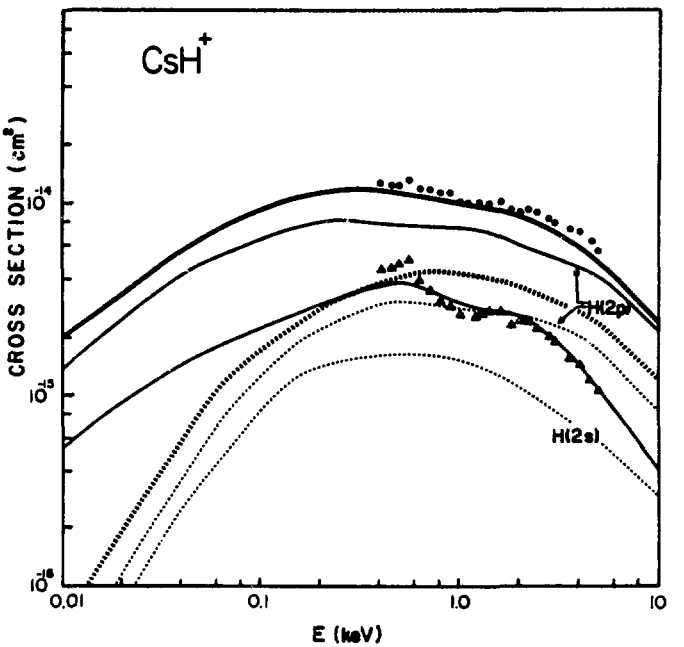

XBL 836-10150

FIGURE 10

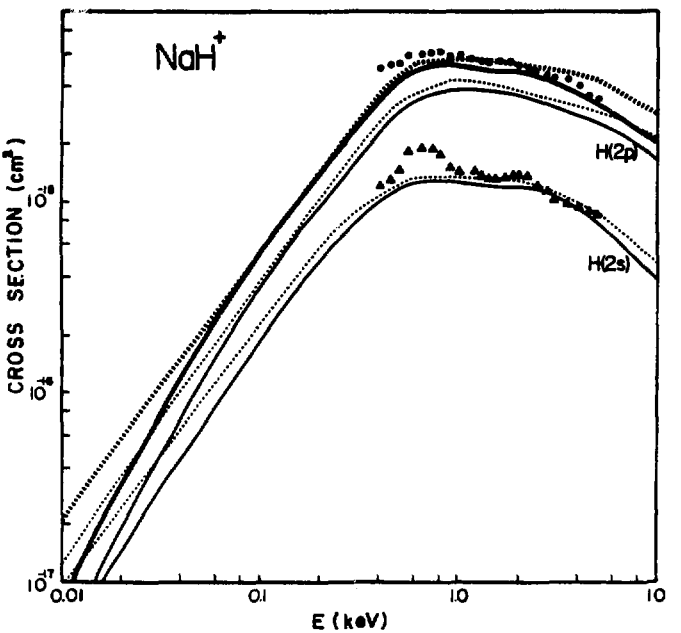

XBL 836-10149

FIGURE 11

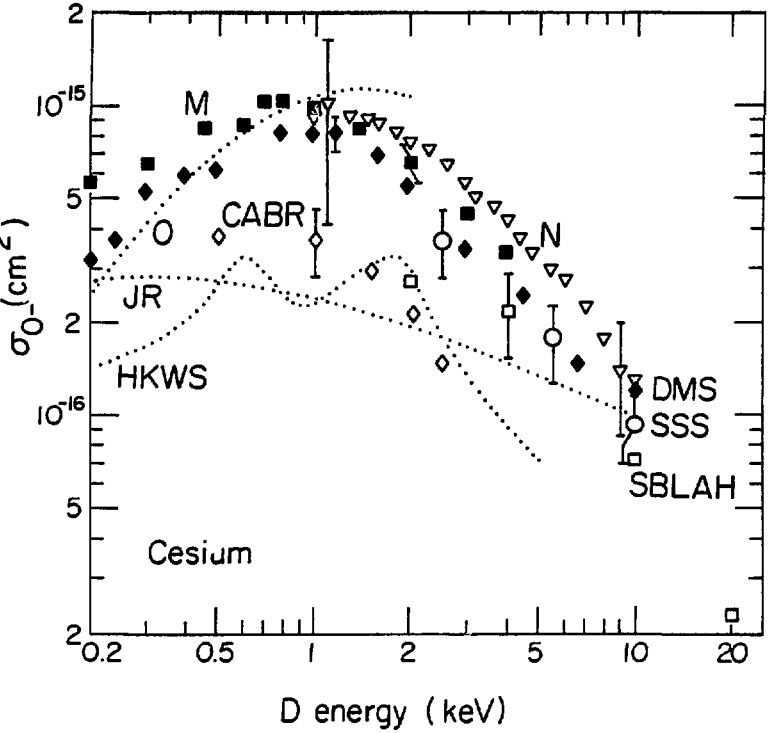

XBL 806-1189A

FIGURE 12

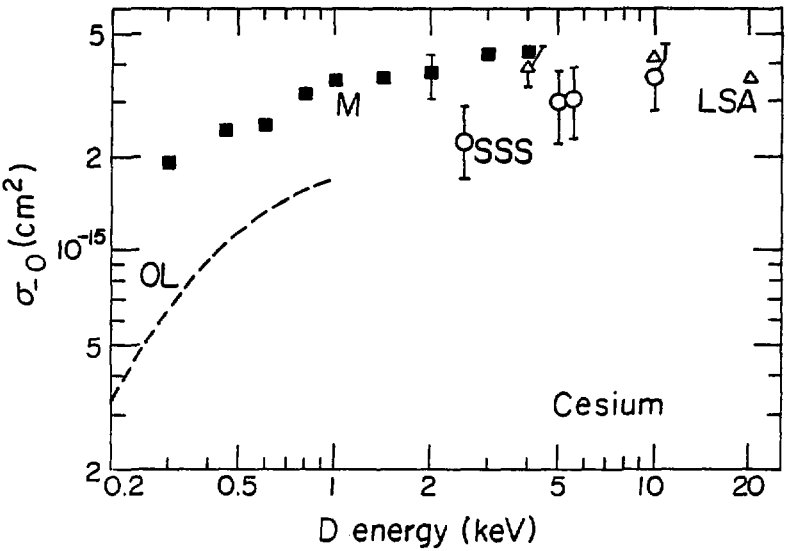

XBL 806-1189B

FIGURE 13

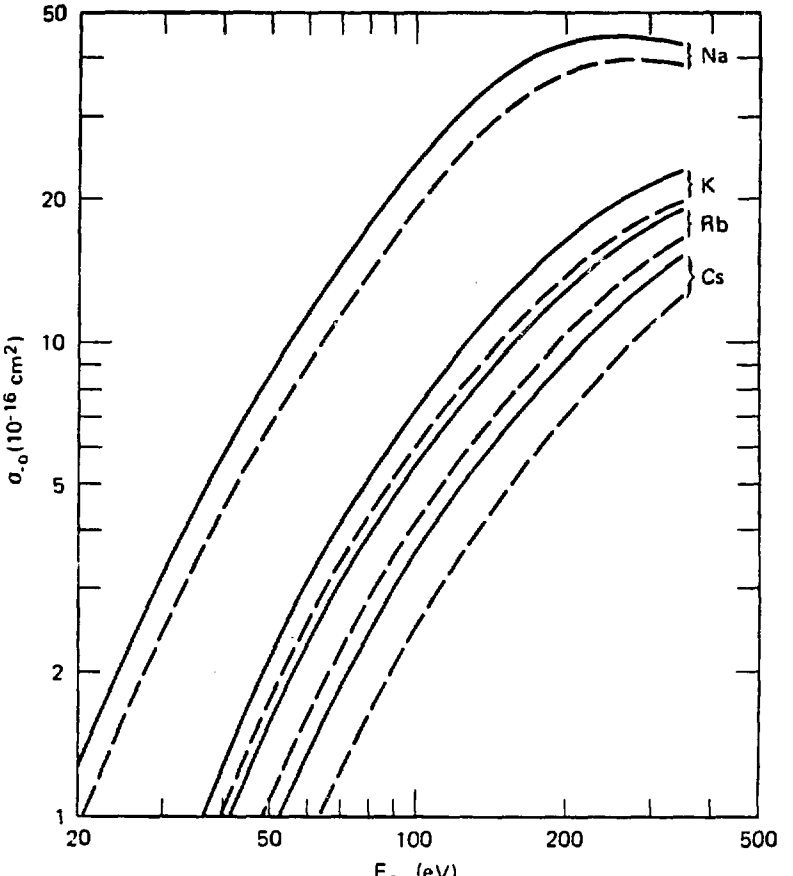

XBL 836-10158

FIGURE 14

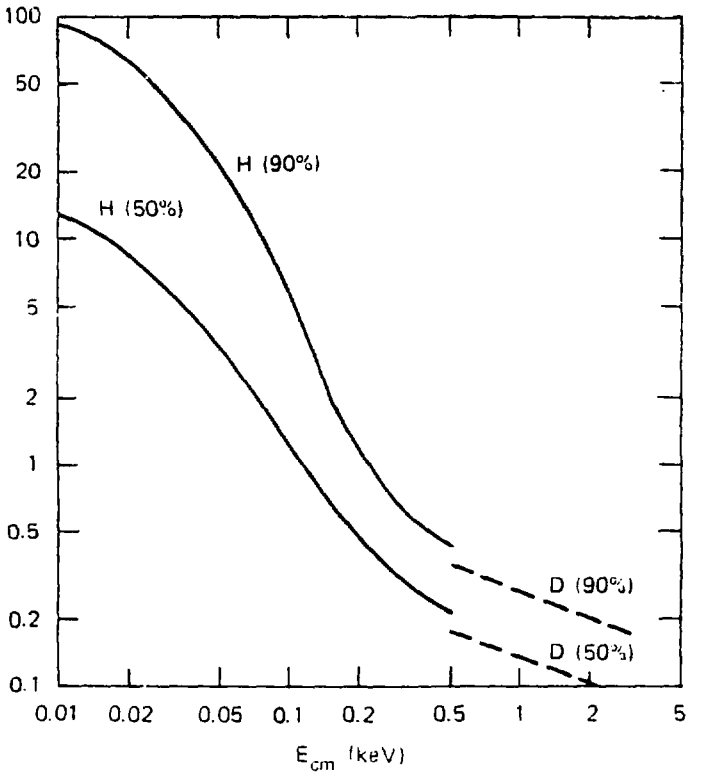

XBL 836-10164

FIGURE 15

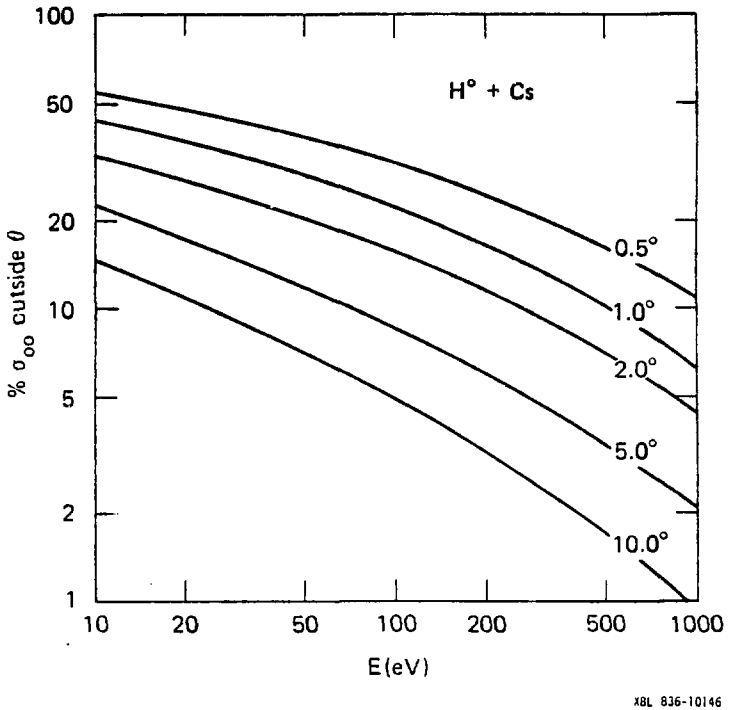
100
50
20
10
5
2
1
% σ_{oo} outside θ
H° + Cs
0.5°
1.0°
2.0°
5.0°
10.0°
10
20
50
100
200
500
1000
E(eV)
XBL 836-10146

FIGURE 16

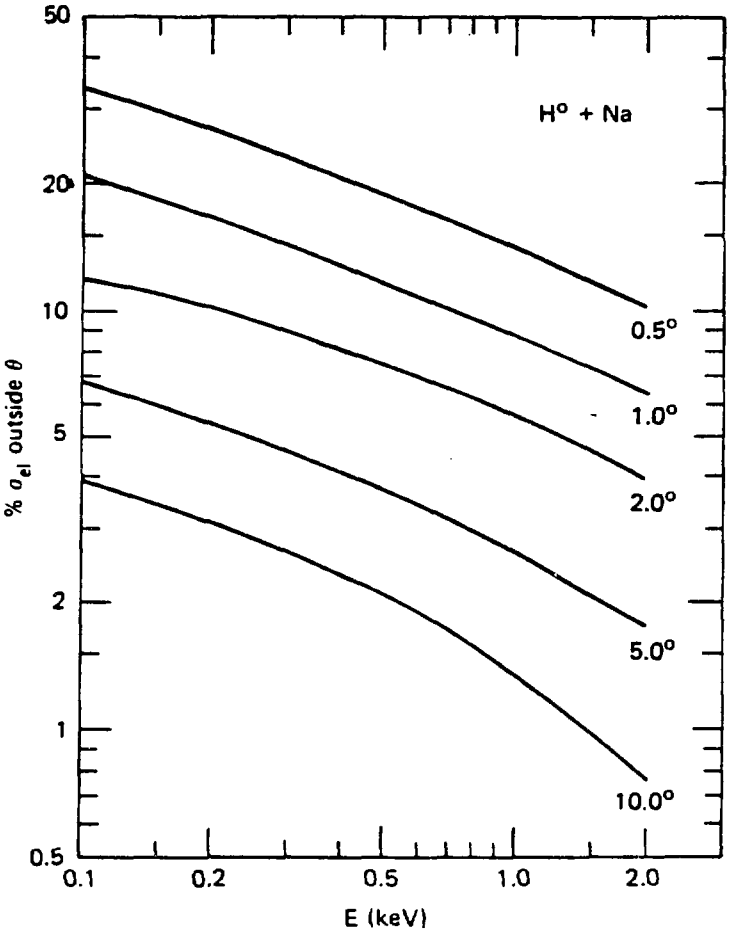

XBL 836-10162

FIGURE 17

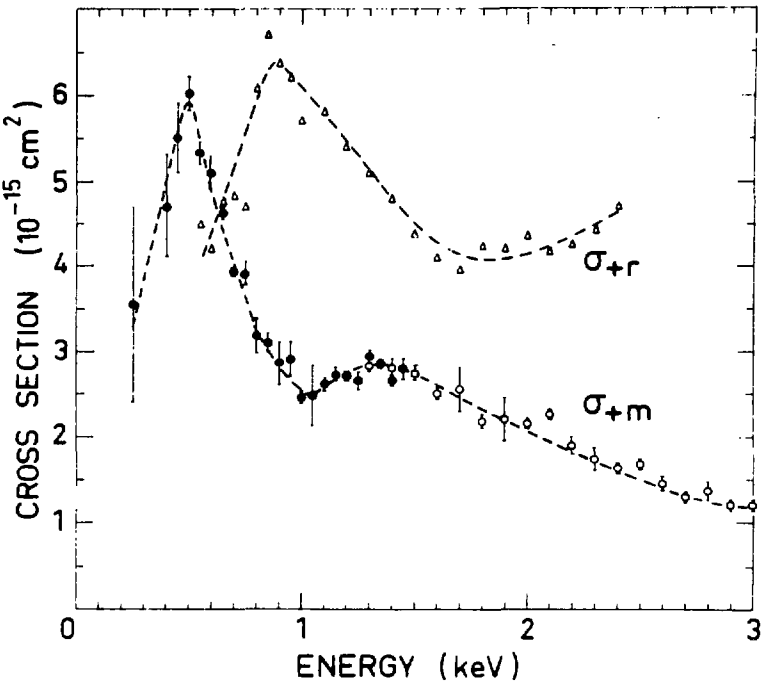

XBL 836-10751

FIGURE 18

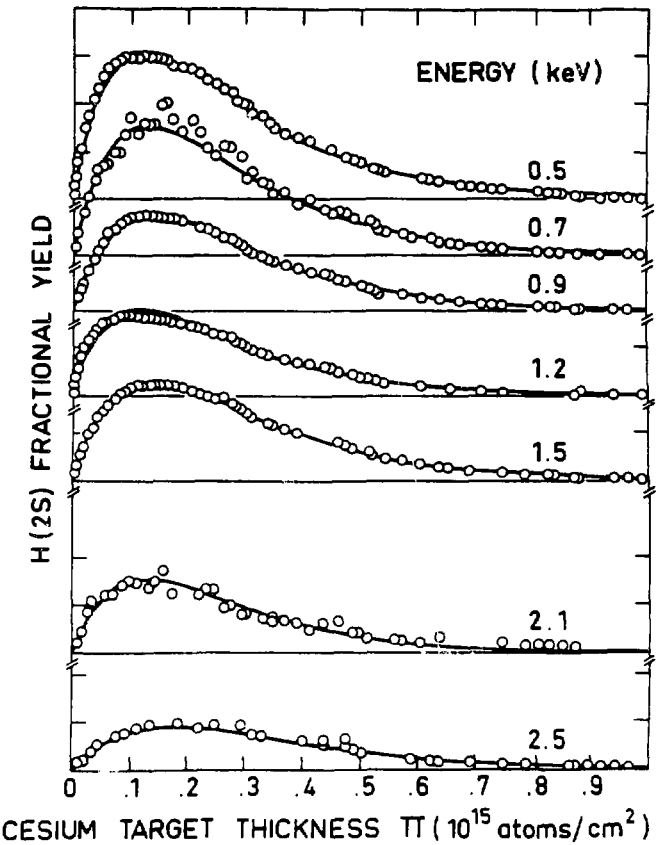

XBL 836-10152

FIGURE 19

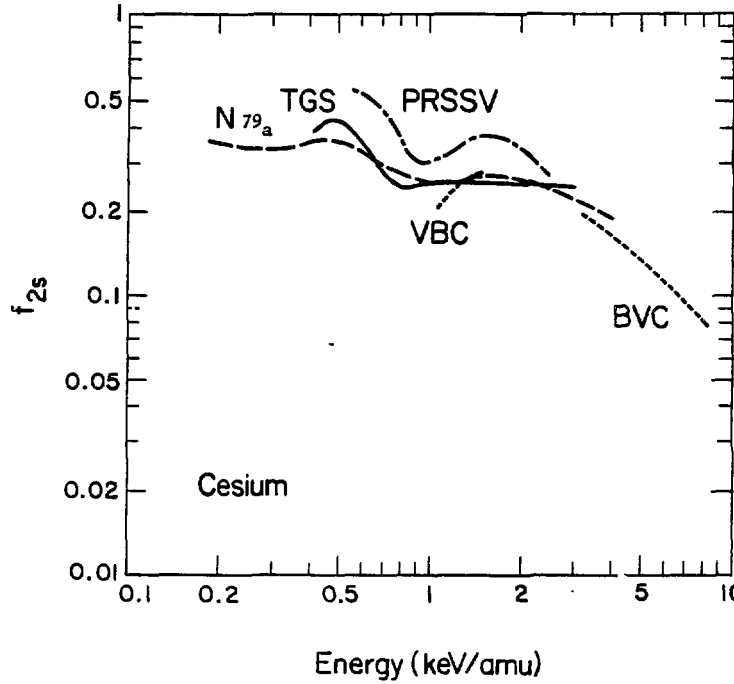

XBL 836-2682

FIGURE 20

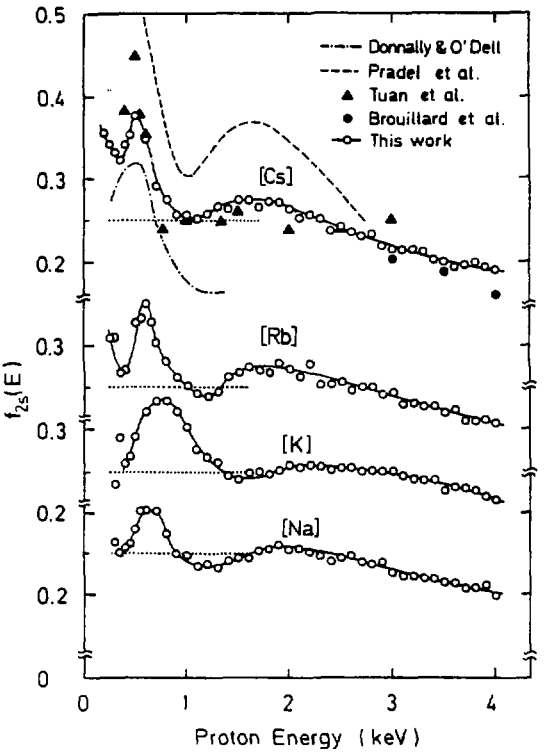

XBL 836-10157

FIGURE 21

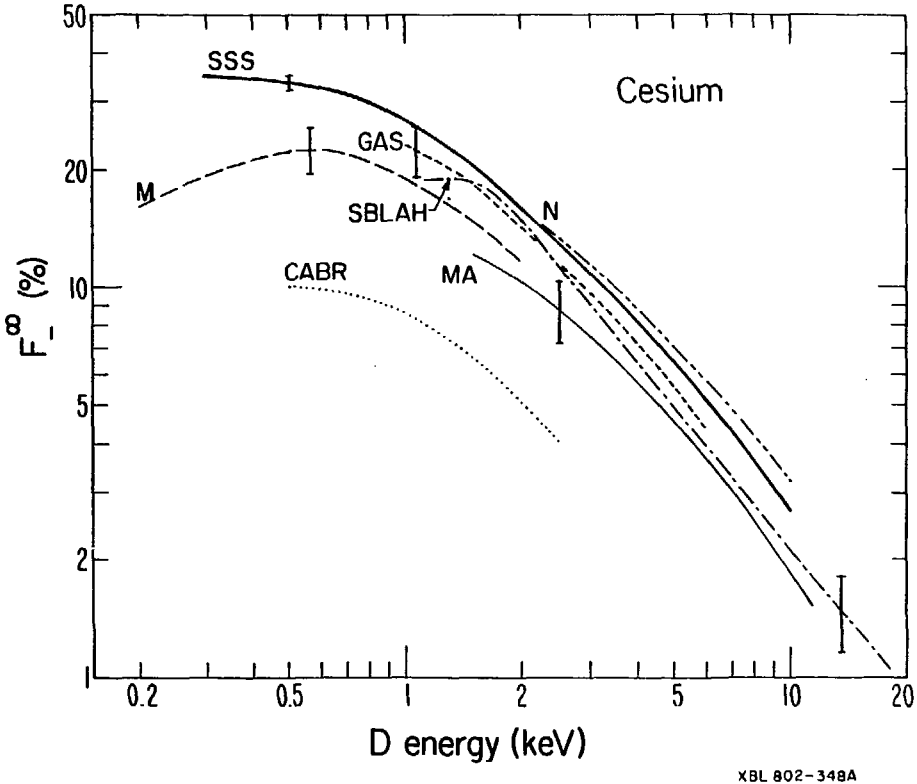
Cesium
SSS
GAS
M
SBLAH
N
CABR
MA
F_{-}^{8} (%)
D energy (keV)
50
20
10
5
2
1
0.2
0.5
1
2
5
10
20
XBL 802-348A

FIGURE 22

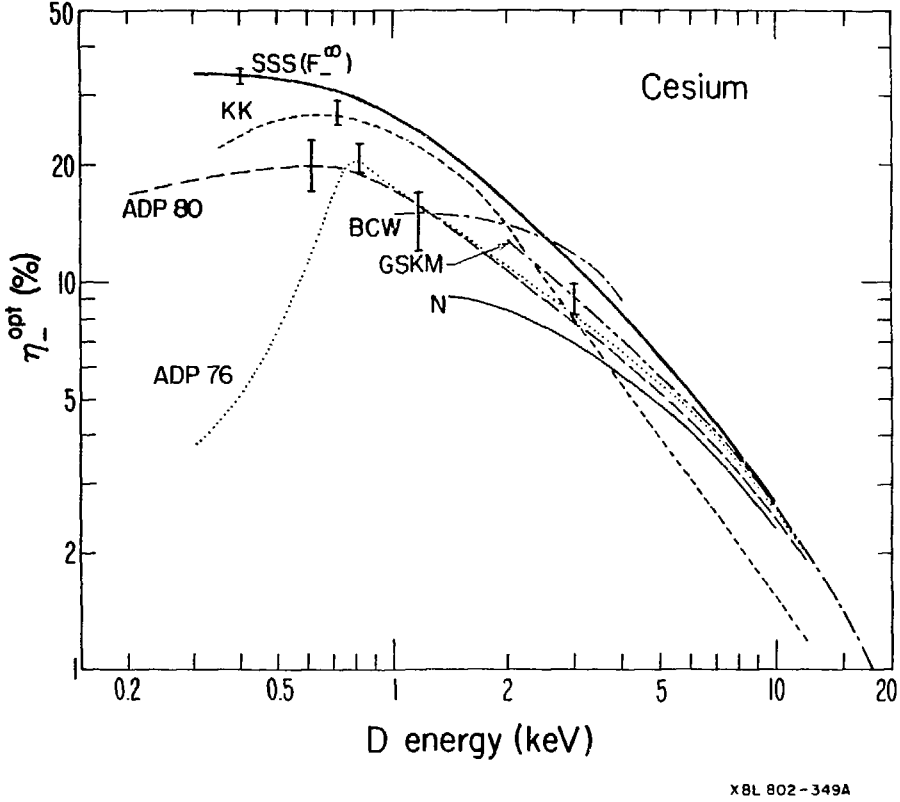

X8L 802-349A

FIGURE 23

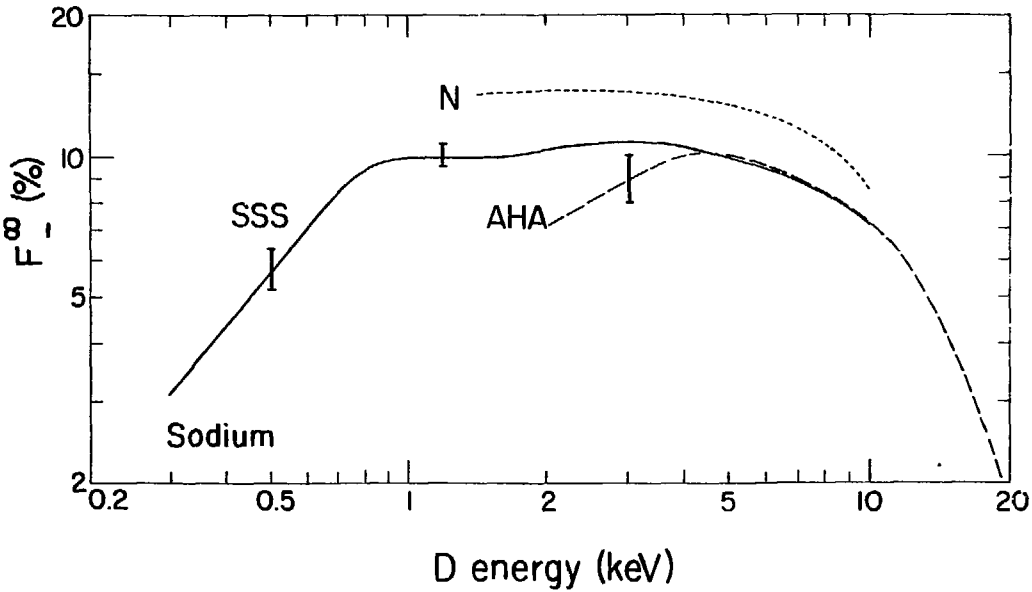

XBL 803-478A

FIGURE 24

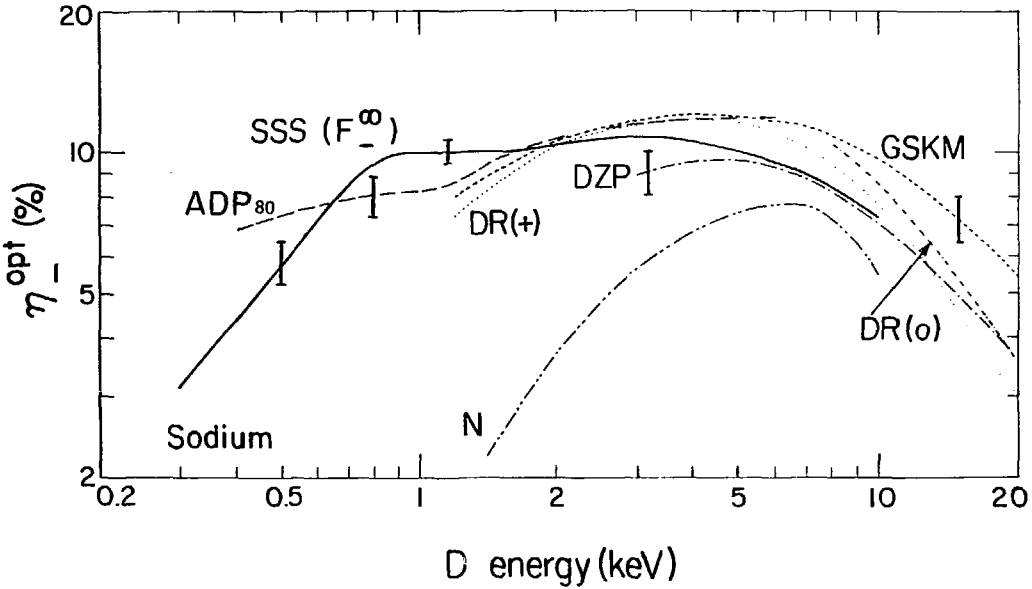

XBL 803-477A

FIGURE 25

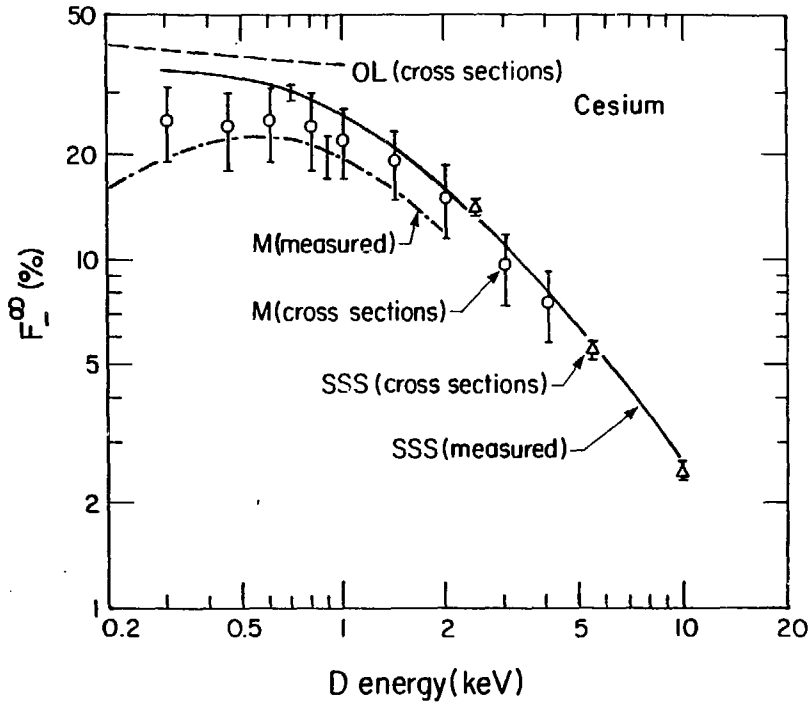

XBL803-468B

FIGURE 26

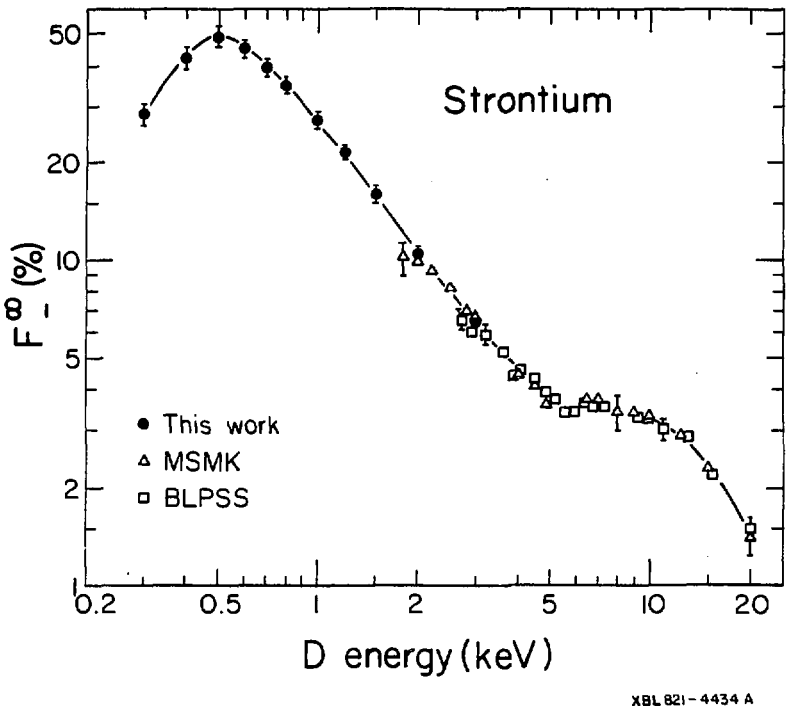
Strontium
50
20
10
5
2
1
F (%)
This work
MSMK
BLPSS
0.2
0.5
1
2
5
10
20
D energy (keV)
XBL 821-4434 A

FIGURE 27

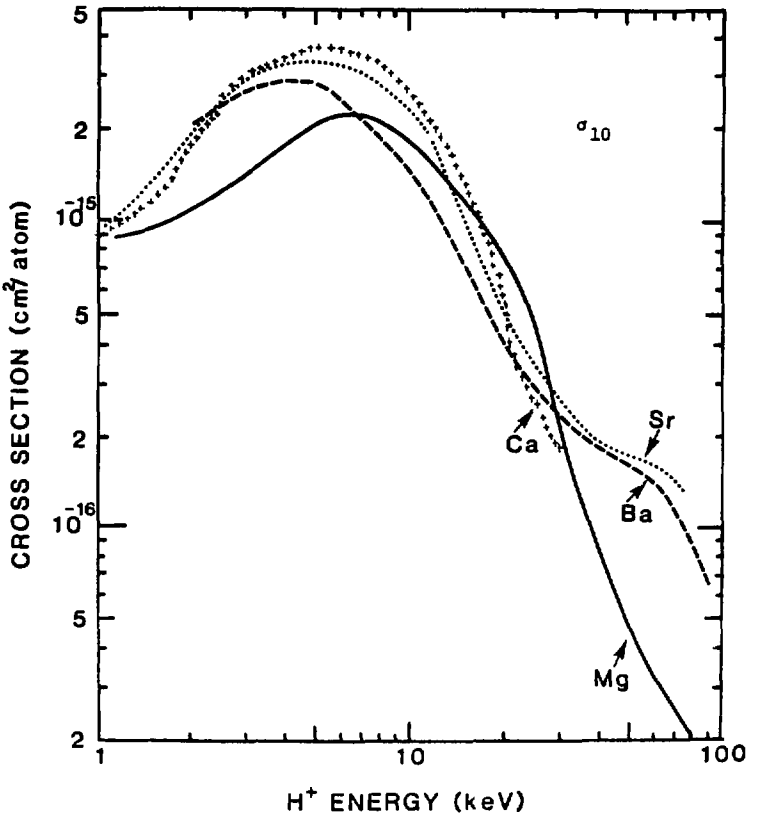
CROSS SECTION (cm² atom)
H⁺ ENERGY (keV)
σ10
Ca
Sr
Ba
Mg
5
2
10⁻¹⁵
5
2
10⁻¹⁶
5
2
1
10
100
XBL 836-10165

FIGURE 28

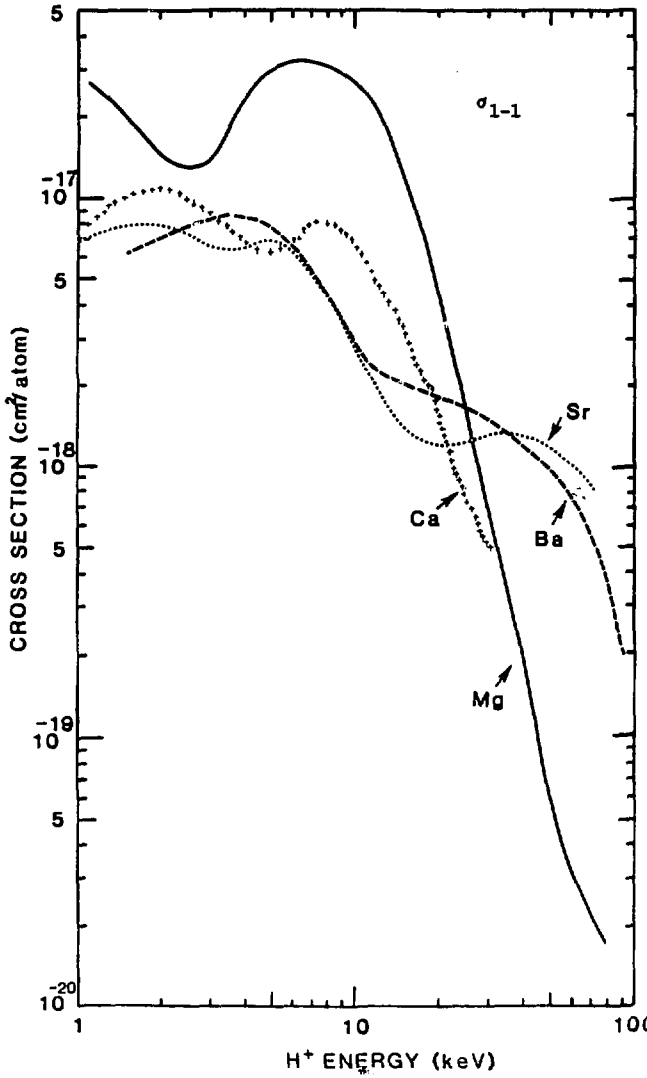

XBL 836-10166

FIGURE 29

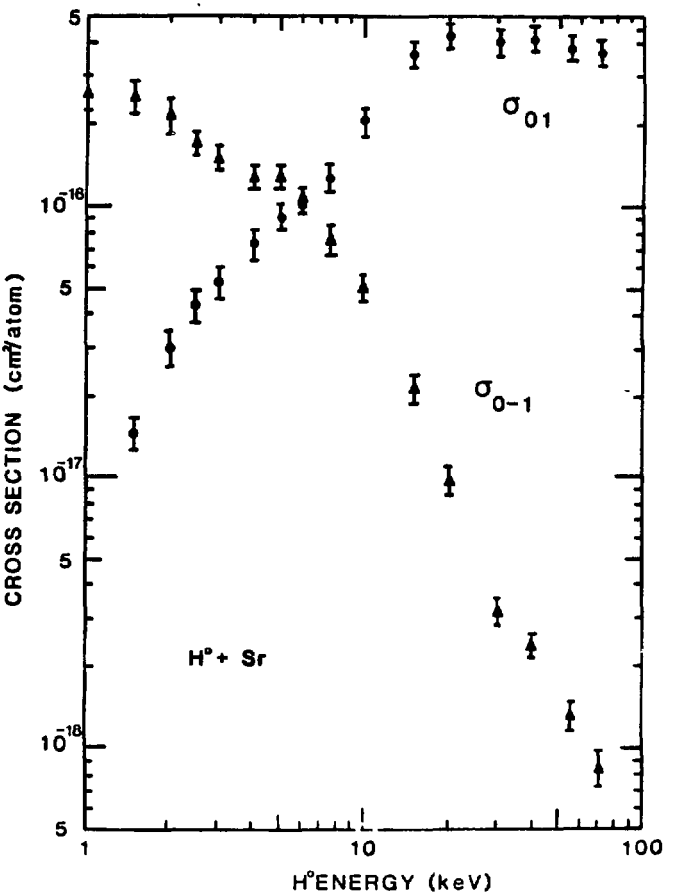

XBL 836-10168

FIGURE 30

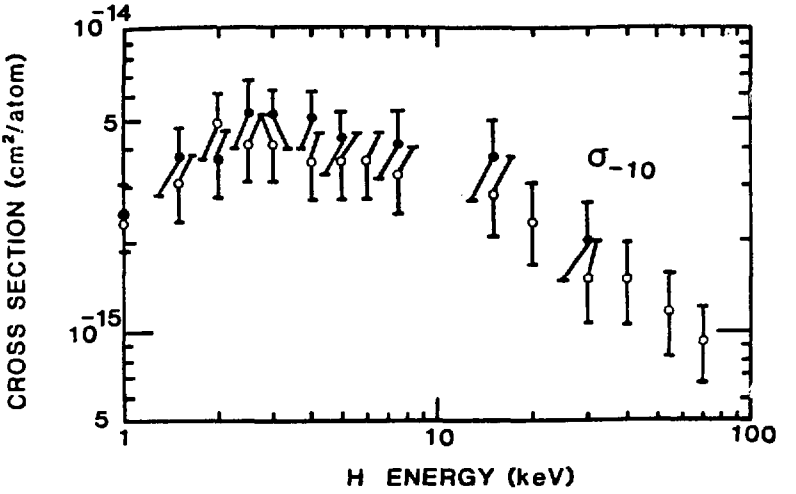

XBL 836-10169

FIGURE 31

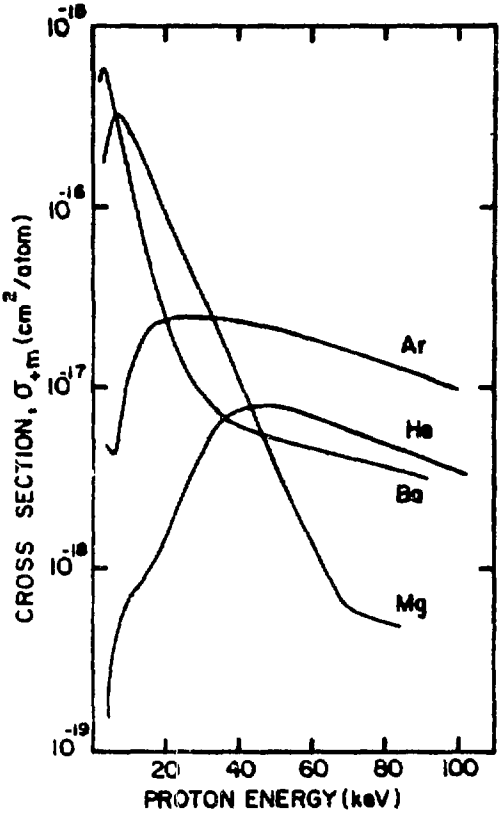

XBL 836-10160

FIGURE 32

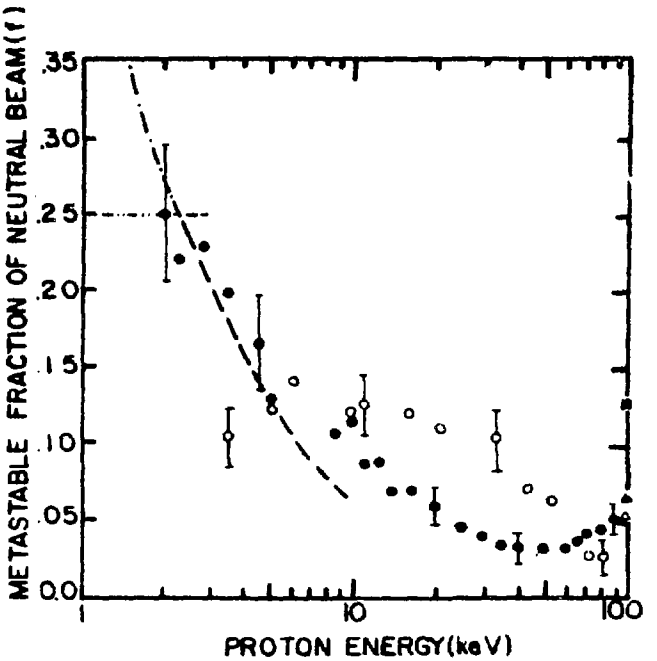

XBL 836-10159

FIGURE 33

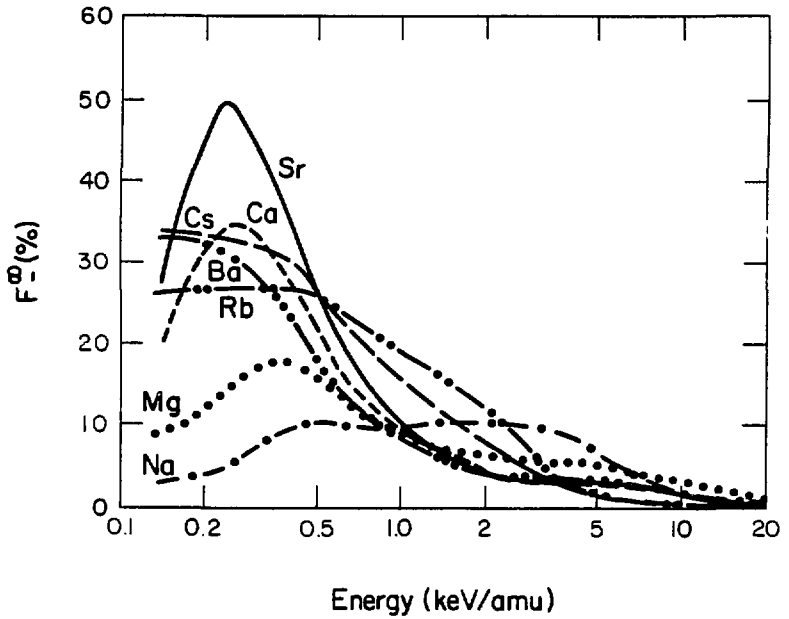

XBL 836-2687

FIGURE 34

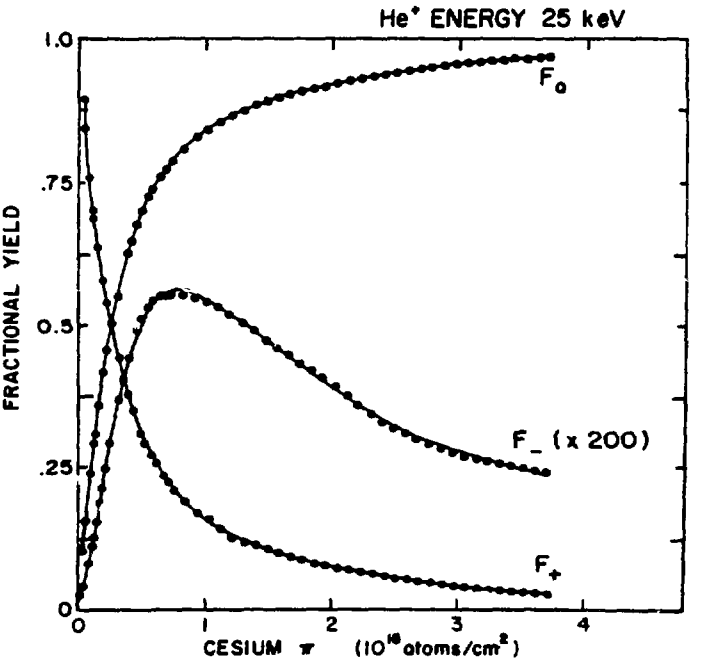

XBL 836-10154

FIGURE 35

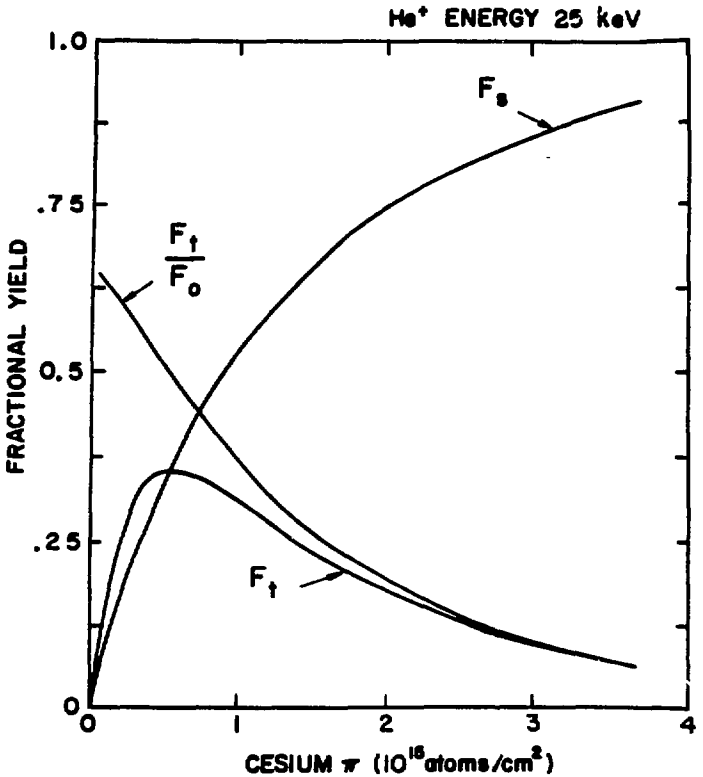

XBL 836-10155

FIGURE 36

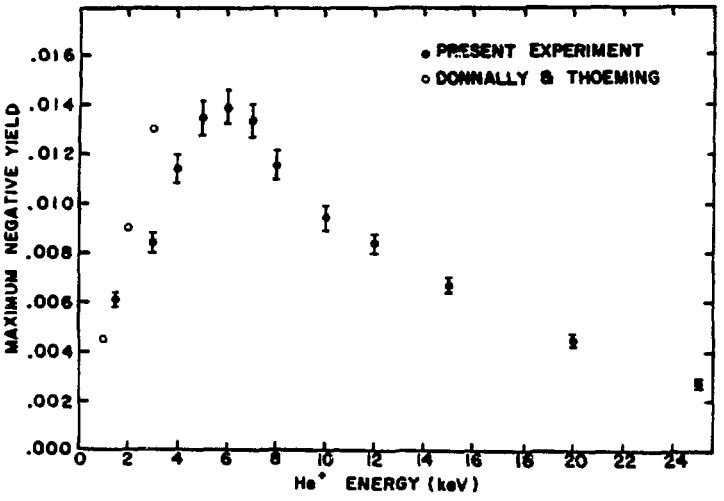

XBL 836-10156

FIGURE 37

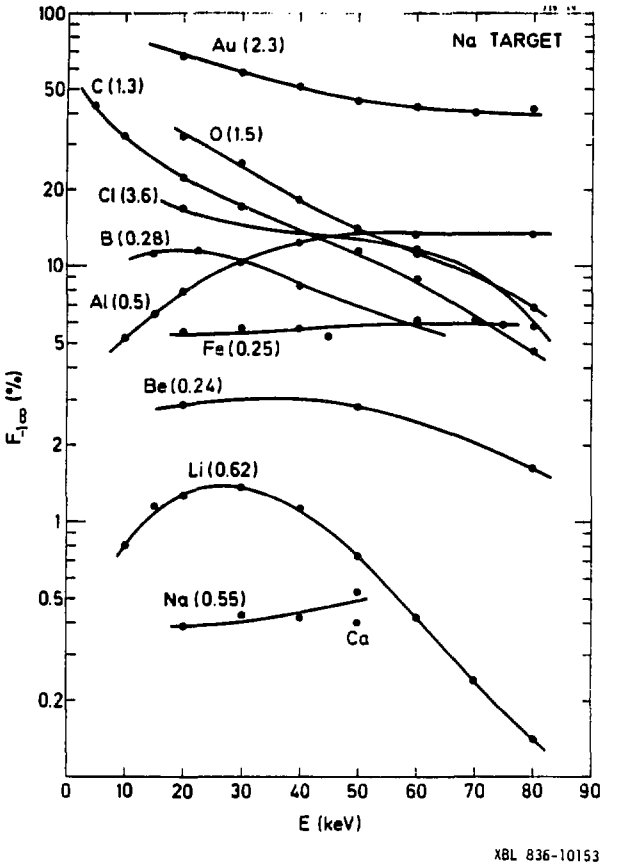
Na TARGET
Au (2.3)
C (1.3)
O (1.5)
Cl (3.6)
B (0.28)
Al (0.5)
Fe (0.25)
Be (0.24)
Li (0.62)
Na (0.55)
Ca
100
50
20
10
5
2
1
0.5
0.2
0
10
20
30
40
50
60
70
80
90
E (keV)
F-1∞ (%)
XBL 836-10153

FIGURE 38

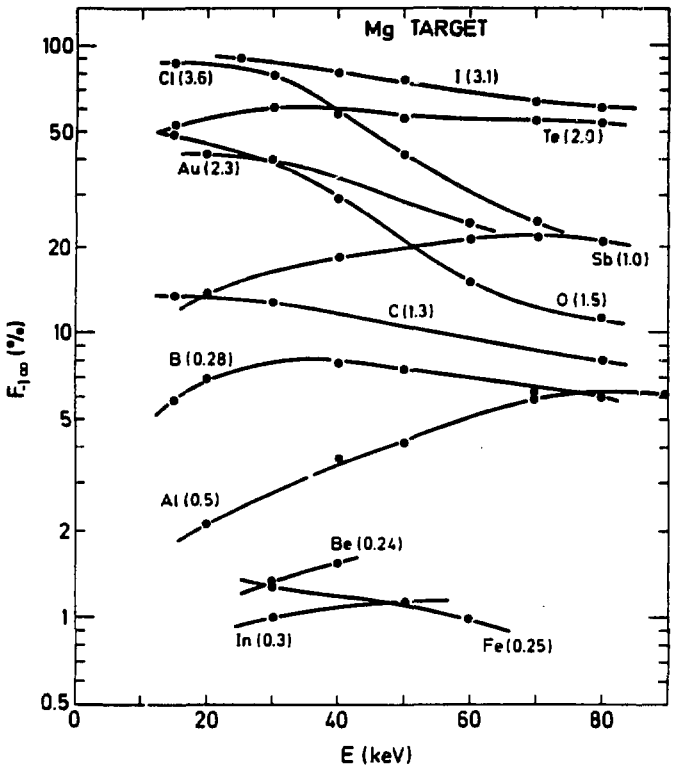

XBL 836-10147

FIGURE 39